Metamaterials & the Meta-6 Layer

Tom Tiwald

For ellipsometry, we usually consider only the electric-field component of the electromagnetic (EM) wave interaction with the material. We ignore the interaction of the wave's magnetic-field component at optical frequencies because atoms and molecules tend to have a weak magnetic response to the rapidly changing fields of EM waves at optical frequencies. Thus we usually consider only *dielectric* response (*permittivity*) and ignore magnetic *permeability*.

However, certain kinds of metamaterials change all of that. Metamaterials consist of an artificially-created array of small structures or particles, usually smaller than the measurement wavelength. These structures or particles can be considered "artificial atoms" or "meta-atoms", with properties tailored to interact with incoming EM waves in ways generally not observed in naturally occurring materials.

The Split Ring Resonator (SRR)

The split ring resonator (SRR) illustrates this point. Each SRR shown in Figure 1 is a miniature inductive-capacitive circuit, with the inductor being a single winding of a wire coil, and the capacitor formed by the gap at the split of the wire[1]. Both Magnetic and Electric components of the incident light interact with the rings.

Current is induced in the ring by *incident H-fields* via the time-dependent magnetic flux enclosed by each ring, and *by incident E-fields* via a voltage drop across the gap surfaces.

At the same time, *the constantly varying current* in the ring *induces a magnetic dipole moment* and *an electric polarization* which interacts with the incident H-fields and E-fields, respectively. The polarization is induced at the gap capacitor, and also by generating time-dependent magnetic fields.

These interactions are frequency (wavelength) dependent with a resonant frequency of $\omega = 1/\sqrt{LC}$. The strength of the resonance partially depends upon the metal resistance, which will dampen the effects. The value of R, L and C depends upon the material properties and dimensions of the SRR.

We can summarize these couplings between the electric field **E**, magnetic field **H**, electric displacement field **D** and the magnetic induction **B** using the constitutive material equations:

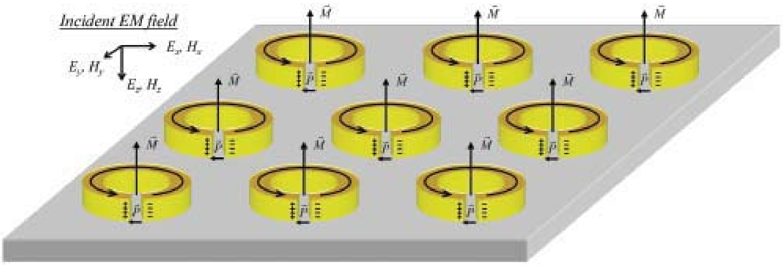

Figure 1. An array of single Split Ring Resonators (SRR's).

$$\mathbf{D} = \varepsilon_o \varepsilon \mathbf{E} + \frac{\gamma}{c}\mathbf{H} \qquad (1)$$

$$\mathbf{B} = \frac{\zeta}{c}\mathbf{E} + \mu_o \mu \mathbf{H} \qquad (2)$$

where c, ε_o, and μ_o are the vacuum speed of light, permittivity, and permeability, respectively. Here, ε is the relative dielectric permittivity and μ is the magnetic permeability; while γ (gamma) and ζ (zeta) are the chiral (or gyrotopic) terms and represent cross-coupling of **H** into **D** and **E** into **B**.

There are other SRR designs, including square rings, u-shapes, etc., as well as two or more rings arranged side-by-side or concentric, or in combination with rods and other elements. Besides SRR's, other geometric arrangements can create time-varying magnetic and electric dipole resonances. These include pillars or rods, crosses, "fishnets", nanorod gratings and other configurations.

Not all metamaterial designs create magnetic dipoles that interact with the incident **H**-fields. Many of the unusual properties can be duplicated or approximated from purely dielectric materials where Re(μ) is either very large or very small, and either positive or negative in value.

Among the unusual optical properties exhibited by metamaterials, perhaps the most frequently discussed is *negative refractive index* (blue box, page 11). Potential applications for metamaterials include frequency-selective surfaces, antenna configurations and invisibility cloaks that hide objects from electromagnetic field probes.

Metamaterial Analysis & Meta-6 Layer

Any complete model of metamaterial structures must be able to model all four relative constitutive functions: ε, μ, γ and ζ from equations (1) and (2). Furthermore, most

Continued on page 10...

...continued from page 5.
metamaterials are anisotropic; and therefore $\boldsymbol{\varepsilon}$, $\boldsymbol{\mu}$, $\boldsymbol{\gamma}$, and $\boldsymbol{\zeta}$ are 3x3 tensors. The constitutive material equations now become

$$\begin{bmatrix} D_x \\ D_y \\ D_z \end{bmatrix} = \varepsilon_0 \begin{bmatrix} \varepsilon_{xx} & \varepsilon_{xy} & \varepsilon_{xz} \\ \varepsilon_{yx} & \varepsilon_{yy} & \varepsilon_{yz} \\ \varepsilon_{zx} & \varepsilon_{zy} & \varepsilon_{zz} \end{bmatrix} \begin{bmatrix} E_x \\ E_y \\ E_z \end{bmatrix} + \frac{1}{c} \begin{bmatrix} \gamma_{xx} & \gamma_{xy} & \gamma_{xz} \\ \gamma_{yx} & \gamma_{yy} & \gamma_{yz} \\ \gamma_{zx} & \gamma_{zy} & \gamma_{zz} \end{bmatrix} \begin{bmatrix} H_x \\ H_y \\ H_z \end{bmatrix} \quad (3)$$

$$\begin{bmatrix} B_x \\ B_y \\ B_z \end{bmatrix} = \frac{1}{c} \begin{bmatrix} \zeta_{xx} & \zeta_{xy} & \zeta_{xz} \\ \zeta_{yx} & \zeta_{yy} & \zeta_{yz} \\ \zeta_{zx} & \zeta_{zy} & \zeta_{zz} \end{bmatrix} \begin{bmatrix} E_x \\ E_y \\ E_z \end{bmatrix} + \mu_0 \begin{bmatrix} \mu_{xx} & \mu_{xy} & \mu_{xz} \\ \mu_{yx} & \mu_{yy} & \mu_{yz} \\ \mu_{zx} & \mu_{zy} & \mu_{zz} \end{bmatrix} \begin{bmatrix} H_x \\ H_y \\ H_z \end{bmatrix} \quad (4)$$

Equations (3) and (4) are embodied in the *Meta-6* layer, which is included in all the newest versions of WVASE32®.

The user can define frequency-dependent functions to describe the various complex dielectric and magnetic properties of the material, as well as any gyrotopic properties.

One restriction: for most accurate modeling, the meta-material should be homogeneous at the wavelengths of interest, (i.e., the dimensions of the "meta-atoms" << λ). When this is not true, the field equations must be solved using numerical finite element methods.

Figure 2 shows the Meta-6 layer along with the four sub-tensors. In this example the gyrotopic tensors are zero.

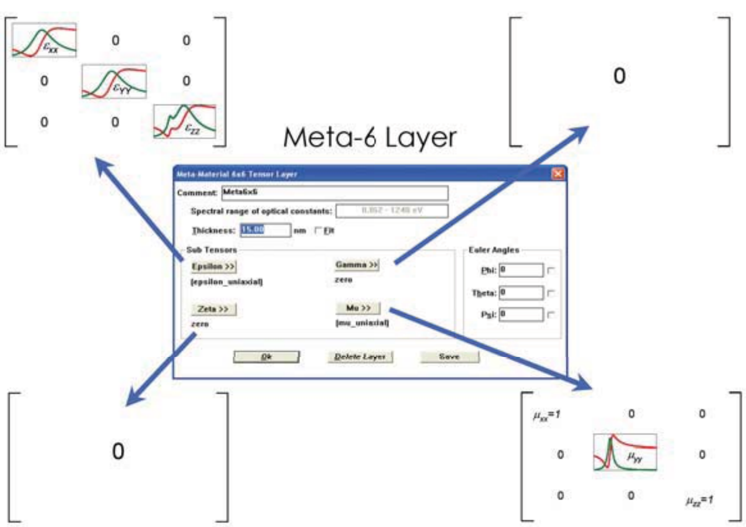

Figure 2. Meta-6 layer and sub-tensors $\boldsymbol{\varepsilon}$, $\boldsymbol{\mu}$, $\boldsymbol{\gamma}$ and $\boldsymbol{\zeta}$. The sub-tensors are defined in separate "dummy layers".

The sub-tensors are defined in separate layers, which are coupled into the Meta-6 layer. This allows the user to define $\boldsymbol{\varepsilon}$, $\boldsymbol{\mu}$, $\boldsymbol{\gamma}$, and $\boldsymbol{\zeta}$ tensor functions using combinations of Genosc, User or other layers.

Gold nanorod simulation

In principle one should be able to produce *LC* resonances at visible frequencies by scaling the SRR geometry to about 100nm. Unfortunately, the maximum operating frequency of that design is limited by the metal resistivity and kinetic inductance[1]. To overcome this, many designs take advantage of the surface plasmons (surface charge density waves) that naturally occur on metal surfaces to produce electric and magnetic resonances at visible wavelengths. The incident EM-wave couples with plasmons on the surface of the metal structures, resulting in a virtual circulating current. The circulating plasmons form magnetic dipoles, which interact with the EM-wave's magnetic-field.

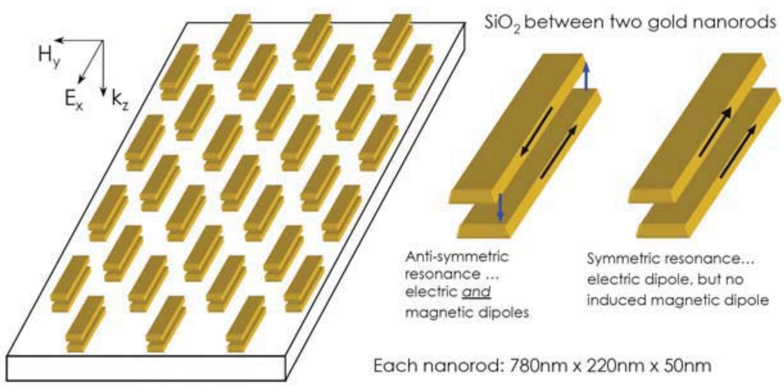

Figure 3. Gold nanorod example. Incident light generates parallel and anti-parallel surface plasmon "current flow" in rods.

An array of gold nanorod pairs (based on a paper by Drachev, et al.[3]) are shown in Figure 3. The E_x-component of incident light introduces horizontal plasmon "currents" in the structures. A symmetric resonance occurs at frequencies where the oscillating E_x-fields cause symmetric plasmon "current" flow in adjacent pillars. An anti-symmetric resonance occurs at frequencies where the oscillating E_x-field supports an anti-symmetric plasmon "current" flow in adjacent pillars. In the dielectric tensor, ε_x will have two Lorentz resonances, symmetric and anti-symmetric, at different frequencies.

Because the anti-symmetric currents mimic a rotational current, a magnetic dipole resonance exists along the y-direction, μ_y. No magnetic dipole exists along the other directions, so $\mu_x = \mu_z = 1$. The permeability tensor would look something like Figure 4.

Figure 5 shows simulated normal-incidence transmission data for the nanorod model. This is only one of many possible data types that can be acquired with an ellipsometer and modeled using the Meta-6 layer.

Metamaterials are usually anisotropic and are often depolarizing; meaning that they usually require either generalized ellipsometry (g-SE) measurements or even Mueller matrix ellipsometry (mm-SE).

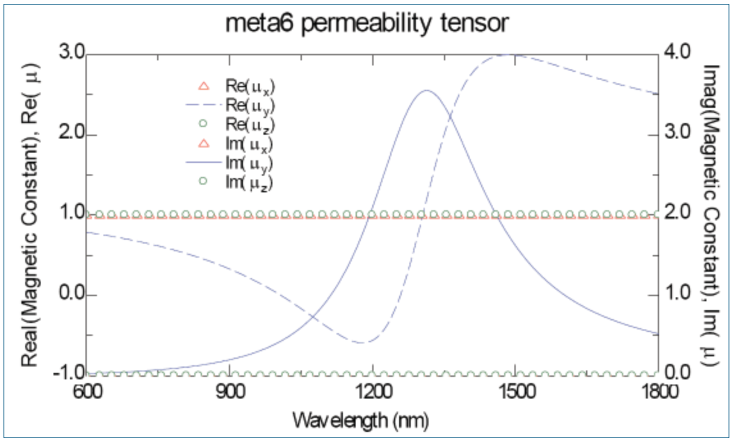

Figure 4. The permeability tensor with magnetic dipole resonance along μ_y.

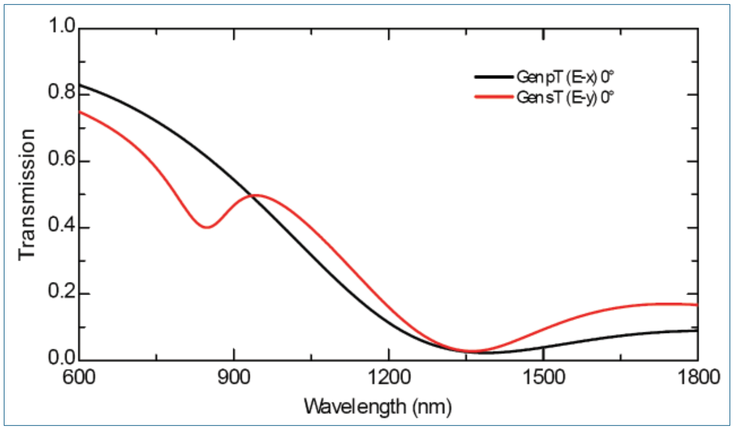

Figure 5. Simulated Transmission for the gold nanorod example.

Negative Index of Refraction

Negative index materials, or NIM's, are metamaterials with a refractive index < 0 over some frequency range. A negative index occurs when both Re(ε) and Re(μ) < 0; therefore materials that possess this property are also called *double-negative* materials (DNM's). Remember that the index $\tilde{n} = \sqrt{\tilde{\varepsilon}\cdot\tilde{\mu}}$. Since ε and μ are generally complex numbers:

$$\tilde{n} = \sqrt{\tilde{\varepsilon}\cdot\tilde{\mu}} = \sqrt{|\varepsilon||\mu|}\,e^{i\left(\frac{\theta_\varepsilon+\theta_\mu}{2}\right)}$$

Veselago[2] showed that when Re(n) < 0; ***E***, ***H***, and the wavevector ***k*** follow a *left-handed* rule instead of the *right-hand* rule, as shown in figure NIM-1. However, the Poynting vector is ***S = E x H***, thus ***k*** and ***S*** can point in opposite directions when light travels through negative index materials. As a consequence, the angle of refraction is negative when n < 0, as predicted by Snell's law. See figure NIM-2.

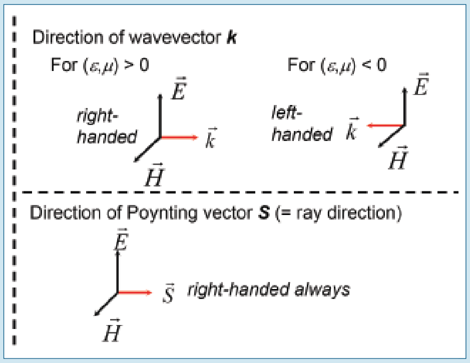

Figure NIM-1. Directions of **k** and **S** for $(\varepsilon,\mu) > 0$ and $(\varepsilon,\mu) < 0$.

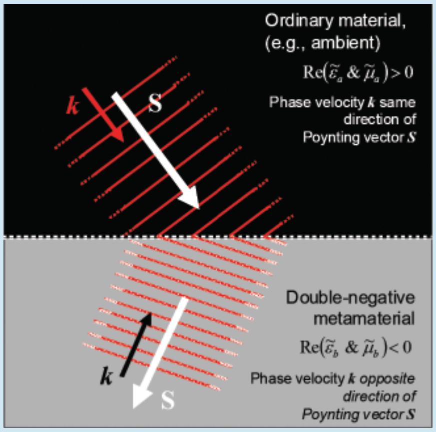

Figure NIM-2. Planes of constant phase (red lines), k and S for light beam entering double-negative material. Angle of refraction is negative, or to the left.

References:

1. M. Wegener and S. Linden, *Physics Today* **63** (October 2010) 32.
2. V.G.Veselago, *Sov. Phys. Usp.* **10**, (1968) 509.
3. V.P. Drachev, W. Cai, U. Chettiar, H.-K. Yuan, A.K. Sarychev, A.V. Kildishev, G. Klimeck, and V.M. Shalaev, *Laser Phys. Lett.* **3**, (2006) 49.